MFM CANOPY REFLECTANCE MODELING AND NORMALIZED BURN RATIO ASSESSMENT OF PRE-FIRE OVERSTORY CANOPY STRUCTURE AND POST-FIRE BURN SEVERITY AT THE LOST CREEK FIRE, ALBERTA ROCKY MOUNTAINS

Derek R. Peddle, Ronald J. Hall, Chris D. Jackson, Scott A. Soenen,
Mark R. Gibb and Daniel T. Juhlin
Department of Geography, University of Lethbridge, 4401 University Drive West
Lethbridge, AB, Canada T1K 3M4
E-mail: derek.peddle@uleth.ca

Ronald J. Hall
Natural Resources Canada, Canadian Forest Service, 5320 – 122 Street
Edmonton, AB, Canada T6H 3S5

ABSTRACT

The Front Range of the Canadian Rocky Mountains has experienced increased wildfire frequency in recent years due, in part, to increasing drought conditions and recreational activity. Mapping the extent and severity of these wildfires is important in forest resources management, with significant environmental, economic and social implications. Forest fires can be a large, rapid source of carbon release to the atmosphere and thus obtaining information such as forest structure and biomass is important for both inventory and studies of carbon cycling and global change. The summer 2003 Lost Creek wildfire in the Crowsnest Pass Alberta Rocky Mountains encompassed a large area in the Montane, Sub-Alpine and Alpine Natural Regions and had a range of severities and overstory conifer fuels. Using near-anniversary pre-fire (Sept. 2002) and post-fire (Sept. 2003) Landsat-5 TM satellite imagery, the fire was first mapped using the differenced Normalised Burn Ratio (dNBR) approach, and compared with the existing fire map available from the Alberta Government Sustainable Resource Development (ASRD). Following this, the Multiple Forward Mode Canopy Reflectance Model (MFM-CRM) inversion algorithm was applied to pre-fire imagery and overlaid fire maps to extract information such as stem density, horizontal and vertical crown radius, and tree height for burned areas identified from both the ASRD and dNBR fire maps. Structural output from this advanced, physically-based algorithm was then used with field allometric relationships to estimate above-ground biomass for both fire products. The total burned area from the Landsat dNBR product was 15,369.48 hectares (ha), considerably less than the 18,966.40 ha from the ASRD map obtained by air photo interpretation. Using MFM-CRM, the percent differences for density, crown radii, tree height and biomass between both fire products ranged from 9.61% to 16.60%. These differences were attributed to the more detailed, per-pixel spatial precision of satellite image analysis and modeling compared to the generalizations inherent with ASRD fire polygons interpreted from aerial photography that were shown to include non-burned areas. These non-burned "islands" may not be of interest for specific source map applications, however, more broadly they represent an inaccuracy that may become significant over large and/or multiple fires at broader scales and for other applications. The effect of this well-known scaling issue was propagated through all outputs and illustrated the importance of avoiding generalisation in fire mapping. Use of satellite imagery provided higher precision over a large area, and further, with MFM physically-based modeling enabled important estimates of structural information and above ground biomass to be derived for both ASRD and satellite dNBR products. The MFM-CRM capability demonstrated here could be used to augment ASRD fire assessments at the Lost Creek fire, as well as for other fires and agency applications elsewhere.

INTRODUCTION

Forest fires play an important role in the environment and in our society. They can threaten urban areas, destroy large amounts of productive timber, affect watersheds and wildlife habitat, and cause loss of life and property (Miller and Yool 2002). They are also a natural and essential component of forest ecosystem succession. When forest fuels burn, significant amounts of carbon can be released rapidly into the atmosphere and thus forest fire information is important to studies involving carbon cycling and global change. In areas such as the Rocky

Mountains, this is particularly important given patterns of drought and other pressures creating higher vulnerability for increased fire frequency, size and intensity (Conrad et al., 2002; Cahoon et al., 1994).

The complexity of forest fires poses significant challenges to mapping and assessment. Fires burn differently depending on characteristics of species, stand attributes and structure (e.g. density, diameter, height, crown dimensions), terrain, moisture, wind, soil type, understory and duff layer, regeneration, ladder fuels (e.g. snags, low lying branches), etc. The resulting non-uniform manner in which fires will burn across the landscape (Weber and Stocks 1998) creates challenges in the estimation of emissions from fires and in determining the uncertainties in which these estimates are made (French et al. 2004). While collection of pre- and post-fire vegetation and fuels information would address many of the challenges and knowledge gaps in assessing fire effects and emissions, the availability of such information is often lacking. As a result, there has been considerable interest in integrating field and remote sensing approaches (Lentile et al. 2006).

Remote sensing has been used extensively for forest fire detection, assessment, and monitoring, ranging from interpretation of aerial photographs to analysis of digital airborne and satellite images (Fraser and Li, 2002; Jia et al., 2006; Lentile et al. 2006), with the latter offering unique advantages in terms of spatial (local to continental; sub-metre to km), spectral (multispectral to hyperspectral; full solar spectrum) and temporal (bi-weekly to daily) attributes. The complexity of fire, together with advances in sensor design and data quality have created new challenges and opportunities for algorithm development to realize the potential of information extraction from remote sensing.

In this paper, Multiple Forward Mode Canopy Reflectance Model inversion (MFM-CRM) of satellite imagery was applied to a forest fire mapping and assessment project, building on previous MFM work involving a variety of forest biophysical-structural applications at different study sites in North America using different airborne and satellite sensors and canopy physical models (Peddle et al., 2003-2007; Soenen et al., 2007abc). Applying this physically-based, advanced modeling algorithm in this context brings new capabilities to forest fire mapping and assessment research. In this study, near-anniversary pre-fire (Sept. 2002) and post-fire (Sept. 2003) Landsat-5 TM imagery were used to: (i) map and compare the fire delineation to the Alberta Sustainable Resource Development (ASRD) fire map, and overlay both maps on the pre- and post-fire imagery; (ii) estimate per-pixel burn severity using the differenced Normalised Burn Ratio (dNBR); (iii) obtain pre-fire, per-pixel structural information (stem density, horizontal and vertical crown radius, height, etc.) using multiple forward mode (MFM) canopy reflectance model (CRM) inversion; (iv) estimate above-ground biomass from MFM-CRM structure and allometric equations and (v) overlay the dNBR and ASRD fire maps on the pre-fire imagery, and compare MFM-CRM structure and biomass for each. In the next section, the two fire maps are described (ASRD, dNBR) and compared, followed by a description of MFM-CRM and its application for providing new information for fire pixels identified from ASRD and dNBR maps. The objectives of the paper are thus to (i) demonstrate some of the capabilities of MFM-CRM in the forest fire context, and (ii) to investigate the importance of proper fire mapping on subsequent structural and biophysical estimates with respect to mapping precision, generalisation and error propagation. One aspect of particular interest for the latter objective is to investigate the spatial magnitude of unburned areas ("islands") within the fire perimeter that are sometimes ignored in the source mapping (in this case, air photo interpretation) context, yet when made available may well be used for a variety of other purposes for which greater accuracy and precision are required, with the concomitant desire to minimise error accumulation across much larger areas.

FOREST FIRE STUDY AREA AND DATA

Lost Creek Fire

The Lost Creek Fire (22 July – 23 August 2003), centered at 49.53°N, 114.48°W, was located on the eastern slopes of the Canadian Rocky Mountains south of Blairmore, Alberta (Figure 1). The fire was started by an unknown event and consumed 18070.1 hectares (ha) as reported by Alberta Sustainable Resource Development (ASRD) Forest Protection Division historical wildfire perimeter document (REF). This fire was significant because of its size in the Rocky Mountains and its proximity to the Municipality of Crowsnest Pass (pop. ~6000). At its peak, the fire burned within 1 km of the town of Blairmore, and less than 1 km from the town of Hillcrest. The fire burned across portions of 3 ecological regions defined by the Montane, Sub-Alpine, and Alpine Natural Regions (Achuff 1992), with elevations ranging from 1296 m to 2194 m asl (mean=1684 m). The dominant overstory coniferous species within the fire extent were lodgepole pine (*Pinus contorta* var. *latifolia* Dougl ex. Loud.), white spruce (*Picea glauca* (Moench) Voss), Engelmann spruce (*Picea engelmannii* Parry ex Engelm.), Douglas-fir (*Pseudotsuga menziesii* (Mirb.) Franco), Balsam fir (*Abies balsamea*), and subalpine fir (*Abies lasiocarpa* (Hook) Nutl.). The dominant deciduous tree species was trembling aspen (*Populus tremuloides* Michx.).
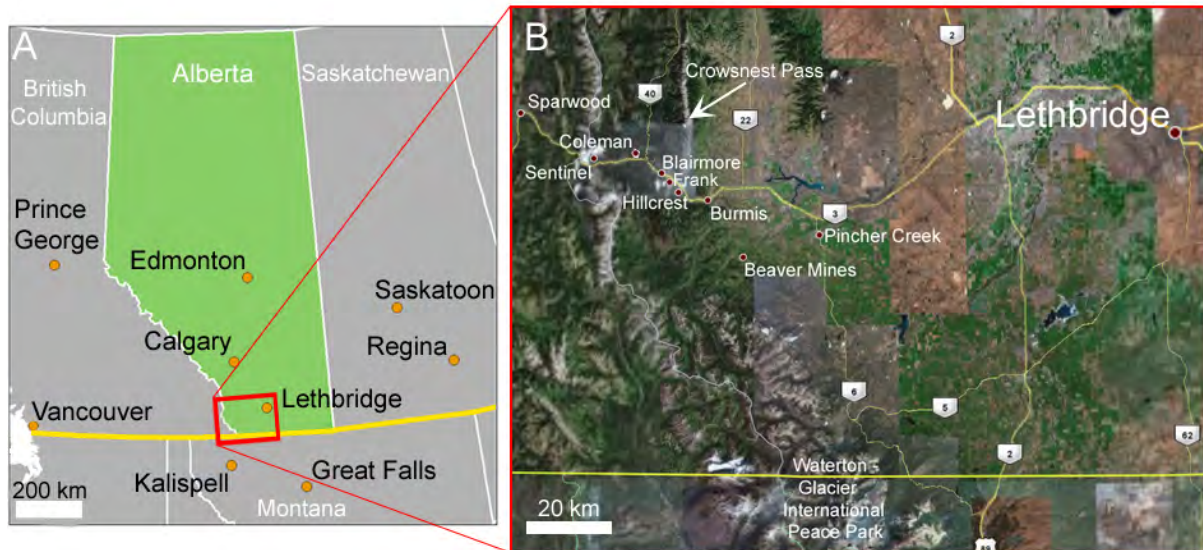
Figure 1. (A): Location of study area in south-western Alberta, Canada. (B) The Lost Creek Fire was located in the Crowsnest Pass area in the north-west quadrant of the image. (Data from Google Maps / Earth).

Satellite Imagery and Topographic Data

Landsat-5 Thematic Mapper (TM) 30 metre resolution imagery were acquired Sept. 11, 2002 and Sept. 30, 2003 (Figure 2). Near-anniversary imagery is desirable for fire mapping and assessment so that vegetation and site conditions would be as similar as possible with respect to seasonal variation. In this case, the post-fire image in the available image pair was acquired 5 weeks after the fire, and thus corresponds to the Initial Assessment (IA) protocols of fire image analysis change detection and burn severity, in contrast to the Extended Assessments that
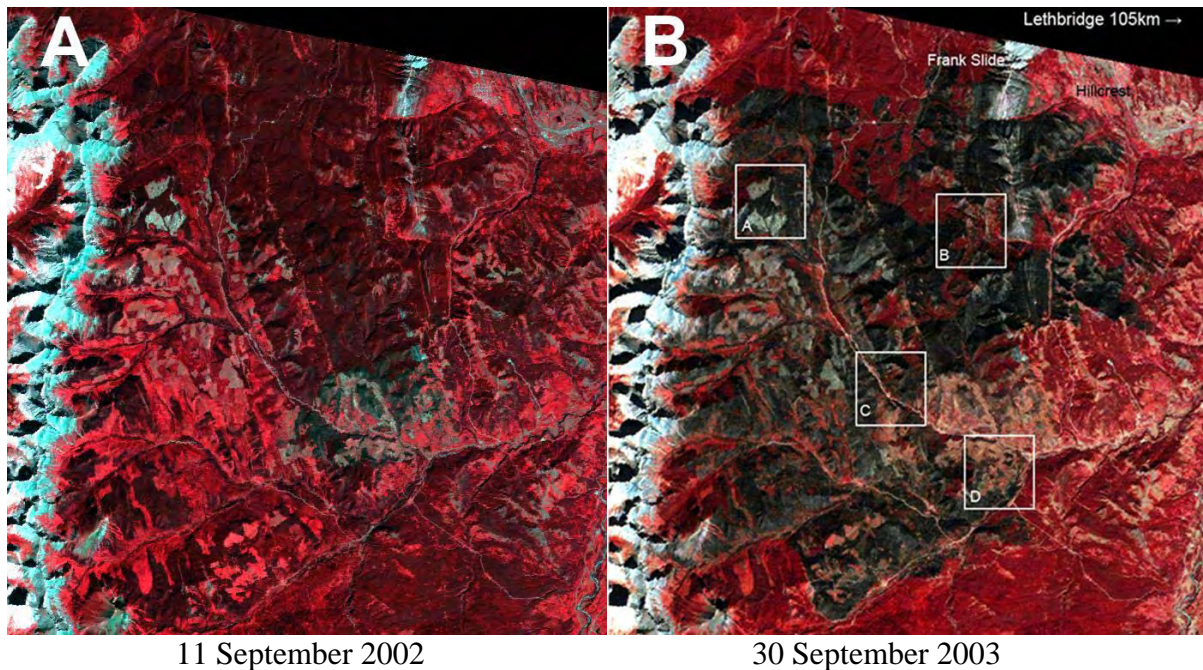

11 September 2002   30 September 2003

Figure 2. Landsat-5 TM imagery for (A) pre-fire and (B,C) post-fire. Bands 4, 3, and 2 (NIR, Red, Green) displayed as RGB, respectively. Boxes A,B,C, D in Figure 2B indicate positions of sub-areas shown in Figure 4. Figure 2C on next page.
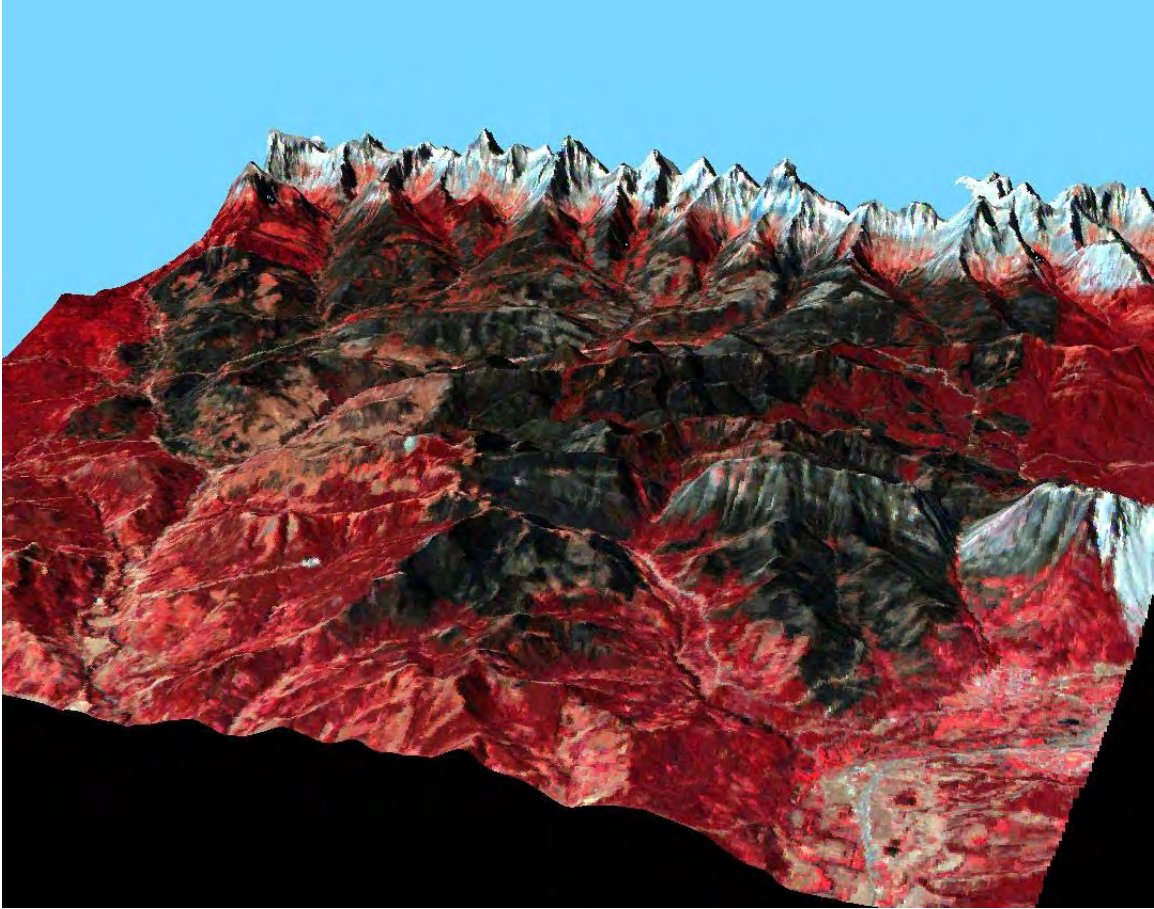
Figure 2C. Landsat-5 TM post-fire image (30 September 2003) draped over digital elevation model (DEM). View from NE, looking west towards the Continental Divide. DEM vertical exaggeration= 2.0. Image bands 4, 3, and 2 (NIR, Red, Green) displayed as RGB, respectively.

FIRE MAPPING AND COMPARISON

ASRD Fire Map

The Forest Protection Division of Alberta Sustainable Resource Development (ASRD) of the Alberta Provincial Government employ several remote sensing methods and image data sources in support of their forest fire management activities. Aerial photography is often used in delineating fire boundaries. Consistent with this approach, for the Lost Creek Fire the available government issued fire map (Figure 3A,B) was based primarily on the interpretation of aerial photography acquired post-fire in 2003 (ASRD, 2006). The positional accuracy of vectors digitized from these interpretations was described as being within ±20m, similar to that of Alberta Vegetation Inventory data (AVI, 2006). Areas of fire were identified and mapped with a general minimum mapping unit within which polygons were generalized. Smaller unburned areas ("islands") are often not considered and thus are often included in the fire class for maps used for stated purposes. However, when these maps are accessed for other applications (e.g. modeling carbon output from a fire), these issues can become important. Accordingly, one objective in this paper was to explore the magnitude and spatial characteristics of this dichotomy.
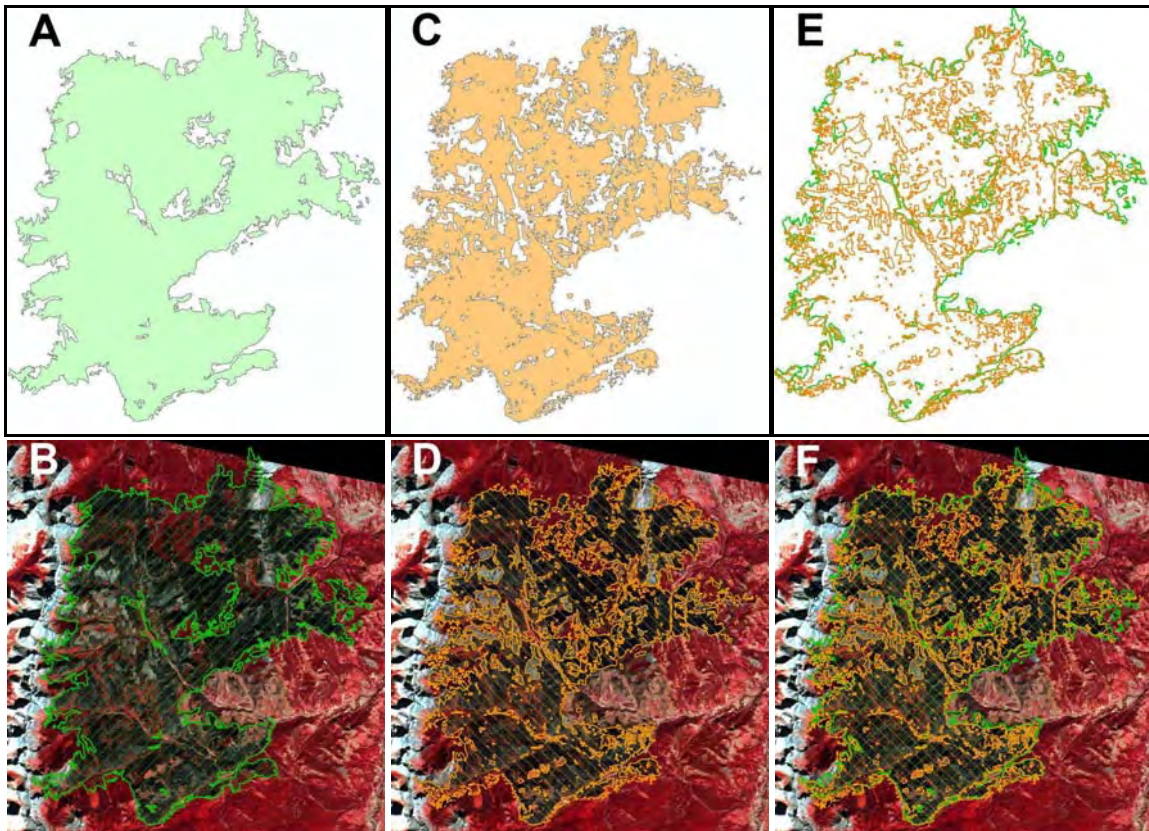
Figure 3. Fire maps shown alone (top) and overlaid on Landsat post-fire image (bottom). A,B: Alberta government ASRD fire map (green); C,D: Landsat dNBR fire map (orange); E,F: ASRD and dNBR maps together.

The ASRD fire map is shown in Figures 3A and 3B. The map is characterized by large, homogenous polygons as a function of the mapping method used and the level of generalization tolerated. When shown over the fire image (Figure 3B), it appears that only relatively larger unburned areas were excluded from the burned map, but that smaller patches of unburned areas were often included in the burn map class. This may be partially a function of time and resource constraints as well as specific product end-use requirements. It is difficult to quantify the spatial threshold of this generalisation because the patterns of inclusion and exclusion appear to vary across the large area. It is unknown if this map was produced with reference to pre-fire information (aerial photography or maps, etc.), however, that may be the case.

Landsat dNBR Fire Map

The differenced Normalized Burn Ratio, or dNBR (Key et al., 2003; Key and Benson, 2006) has been used extensively in the United States for operational forest fire mapping and for providing an index of burn severity. The method is highly sensitive to change in vegetation from pre-fire versus post-fire imagery, and was recommended by Brewer et al. (2005) in a comparison of six methods for classification and mapping of wildfire severity. NBR is computed for a given image using top of the atmosphere (at-sensor) reflectance derived from Landsat TM (or ETM+) band 4 (NIR: 780-900nm) and band 7 (SWIR: 2090-2350nm). These bands have the greatest differences in response to fire damaged vegetation, but in opposite directions (after a fire, band 4 decreases whereas band 7 increases). NBR is computed for each image (pre-fire, post-fire) using the equation (similar to NDVI):

$$\text{NBR} = (\text{Band 4} - \text{Band 7}) \ / \ (\text{Band 4} + \text{Band 7}) \quad (1)$$

The final dNBR (differenced NBR, sometimes also called delta NBR or ΔNBR) is derived as:

$$\text{dNBR} = \text{NBR}prefire - \text{NBR}postfire \quad (2)$$

The dNBR provides a useful indicator of both fire extent and burn severity (Key et al., 2003; Key and Benson, 2006). In addition to burn severity, the dNBR method can also indicate areas of enhanced regrowth in which post-fire vegetation recovery and regeneration was accelerated compared to typical seasonal patterns (i.e. no fire: Key et al., 2003). The resulting dNBR values can be categorized into classes based on dNBR ranges (e.g. unburned, enhanced regrowth, low, moderate, high severity), however, these are specific to scene-pairs and benefit from field information (Key and Benson, 2006). In this study, it was not possible to categorise dNBR and instead the original dNBR values are presented.

The Landsat dNBR fire map is shown in Figures 3C and 3D. The map is characterized by considerable detail for an area this size, and which is consistent through the area corresponding to the Landsat TM 30m pixel spatial resolution. At each pixel, NBR is derived consistently using known and quantitative criteria, with the results from the pre-fire and post-fire imagery combined rigorously and explicitly in the final dNBR product shown. With reference to Figure 3D, the map appears to bear strong correspondence to burned and non-burned areas based on visual inspection (the reader is encouraged to enlarge all Figures in this paper when viewed digitally).

Comparison of ASRD and dNBR Fire Maps

The two map products were compared both visually in Figure 3 (full area) and Figure 4 (close-ups) and also with respect to total burned area (Table 1). The burn perimeter from both products (Figure 3E,3F) appears to have good correspondence, with only few exceptions such as the NE part of the area near the Frank Slide mapped as burned in ASRD but not by dNBR. The main differences between the two products were observed within the fire perimeter. These were attributed largely to the purpose of provincial fire maps to capture the areal extent of burned areas. The dNBR map has considerably more detail in terms of small non-burned areas that were excluded from the burn class but included within larger burn polygons in the ASRD map (Figure 3E, 3F). This results in a distinctively more irregular and detailed appearance with the dNBR product compared to the larger, perhaps aesthetically more pleasing ASRD polygons. However, comparing the smaller polygons internal to the fire perimeter in Figure 3D (dNBR) with the corresponding areas in Figure 3B (ASRD) shows immediately that the dNBR method has accurately identified smaller unburned areas. This is illustrated in Figure 4 that shows four examples of unburned areas being mislabeled as burned in the more generalized ASRD polygons. These errors appear to be due primarily to the considerably more coarse level of detail and its inherent generalisation, however, other features such as cutblocks, roads and other relatively static features were misclassified as burn. The rigorous, explicit method of capturing vegetation change as characterized by fire disturbance from pre- and post-fire NBR products drives this result. Further, in terms of non-fire disturbance and change, the success of the dNBR method is attributed to the unique sensitivity of the Landsat NIR and SWIR bands selected that respond in unique and well established and predictable ways to fire versus other disturbance. This, coupled with the reasonably high spatial resolution (30m) that is applied over large areas gives rise to an effective fire mapping protocol.

Table 1. Area and pixel count for ASRD vs. Landsat dNBR fire maps.

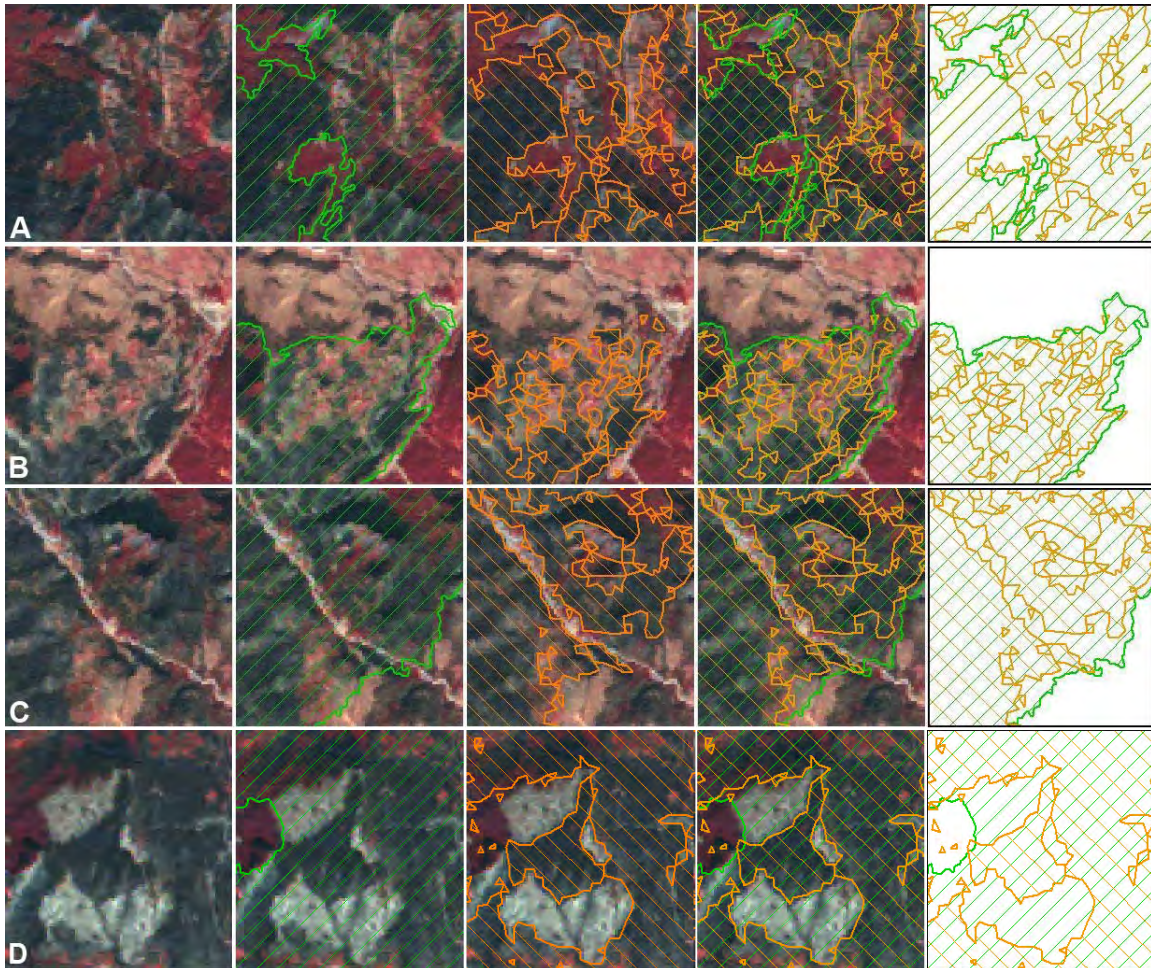| Method	Area (ha)	# Pixels
ASRD	18,966.40	211,499
Landsat dNBR	15,369.48	171,926
Difference:	3,596.92	39,573

Figure 4. Example sub-areas showing differences in ASRD and dNBR products (locations of each set A-D shown in Figure 2B). Left to right: fire image alone; with ASRD boundaries (green); with Landsat dNBR boundaries (orange); with both boundaries; both boundaries alone.

In terms of fire area (Table 1), and consistent with the visual assessments, the dNBR fire area is considerably less than the ASRD fire area, by over 3500 ha. From Figure 3, it is interesting to note that there appear to be few, if any ASRD burned pixels that were mislabeled as unburned in the dNBR product. This is consistent with the contrasting spatial arrangement and internal homogeneity produced by these very different fire mapping approaches. Thus, virtually all differences in area are attributed to unburned area being misclassified by ASRD as burned (i.e. included in large, 'burn' polygons). Over 39,500 Landsat TM pixels were so affected. This amount and area of misclassification is potentially significant with regard to the various uses of fire maps and reports based on them.

MFM-CRM STRUCTURAL AND BIOMASS ESTIMATES

Multiple Forward Mode Canopy Reflectance Modeling of Forest Structure

The pre-fire Landsat image was used to obtain forest biophysical structural information using a canopy reflectance model (CRM) approach applied to the fire maps obtained from the post-fire Landsat image. Multiple Forward Mode (MFM) canopy reflectance model (CRM) inversion (Peddle et al., 2003, 2007) was used with the Geometric Optical Mutual Shadowing (GOMS) CRM (Li and Strahler 1992) to obtain species, stand density, horizontal and vertical crown dimension, height to crown center, and tree height information. This CRM method works by modeling the structure, view, illumination and surface terrain geometry, and the spectral properties of sub-pixel scale scene components that together contribute to the overall, pixel level reflectance received by an airborne

or satellite (e.g. Landsat) sensor. When run in MFM, the model generates a series of candidate reflectance values in a look-up table (MFM-LUT), with each entry possessing the full set of structural and other inputs used. All possible combinations are modeled, with pre-set or automatically derived (e.g. no field or other data) minimum and maximum values with increments (see Table 2). At each Landsat pixel, the multispectral satellite band values are searched in the MFM-LUT for matches. Once the search has been successfully resolved (Peddle et al., 2004; Soenen et al., 2007b), the structural values associated with the modeled reflectance value that matches the satellite reflectance value is then output as the set of structural estimates.

This MFM-CRM approach has been applied successfully with the Canada Centre for Remote Sensing, Canadian Forest Service, Canadian Model Forests, Alberta Ingenuity Centre for Water Research, and in the USA by the NASA MODIS Science Team and the Landsat Ecosystem Disturbance Adaptive Processing System (LEDAPS) as part of NASA's contribution to the North American Carbon Program (NACP, 2005; Cihlar *et al.,* 2002). In these and other projects, MFM has been used for land cover, biomass, stand and crown volume, stem density, height, LAI, topographic correction and validation, structural change detection and damage assessment, crown closure, and water / hydrology applications in different locations and ecosystems in Canada (six provinces from Newfoundland to British Columbia) and USA (MODIS and LEDAPS validation sites) using different canopy reflectance models coupled with MFM (e.g. GOMS, GORT, 4-Scale, 5-Scale) and with a variety of airborne and satellite remote sensing systems (e.g. SPOT, Landsat TM/ETM, MODIS, IKONOS, airborne MSV, casi, Probe-1, AISA), as described in Peddle *et al.* (2007, 2004, 2003abc), Soenen *et al.* (2007abc, 2005), and Pilger *et al.* (2003), with broader perspectives on MFM provided in Cihlar *et al.* (2003) and Gamon *et al.* (2004).

Based on the MFM-CRM structural inputs (Table 2), matches were obtained at each pixel for density (λ), horizontal (r) and vertical (b) crown radius, height to crown center (h) and height distribution (dh), from which tree height was derived (h+b). Biomass was then derived based on the structure and field information described above. Values of density and tree height appear higher towards the N and NE portions of the fire (Figure 5A-D), as well as in smaller pockets in the SW.

Table 2. MFM-CRM inputs. These can be derived automatically by the MFM algorithm if no *a priori* field data are available.

MFM-CRM Parameter	*Min*	*Max*	*Step*
Density: λ (stems/ha)	500	5500	1000
Horizontal Crown Radius: r (m)	1	5	1
Vertical Crown Radius: b (m)	1	7	1
Height to Crown Center: h (m)	5	15	5
Height Distribution: dh (m)	5	20	5
Size of parameter set:			2520

MFM-CRM Biomass Estimates

Biomass estimates were derived using a regression model created to relate *r* and *b* parameters, summarized as crown surface area (SA), to tree biomass for stands at Kananaskis AB (Soenen et al., 2007c), a similar Rocky Mountain environment north of the Lost Creek fire. Crown SA was related to biomass as an analogue to the area of crown supporting physiological processes. SA-based tree biomass allometric equations were adapted from Soenen et al (2007c) using linear least squares regression driven by field measurements of crown dimensions (*r, b*) and previous calculations of tree biomass from a dbh-based log-transformed power model for sampled trees. The SA-based allometric equations were then applied to predict average per-pixel tree biomass, which was then aggregated to total biomass by multiplying the estimate of λ by the average tree biomass. The result was a set of biomass solutions that were resolved using a median-value solution set approach after Weiss et al. (2000). The biomass patterns (Figure 5G,H), as expected, followed the spatial patterns of the MFM-CRM structural parameters used in the biomass procedure. The highest biomass values were found in the N and NE parts of the study area, with smaller areas of high values in the SE. Intermediate biomass values were also found in parts of the central and west-central areas, possibly driven by some of the high r values there.
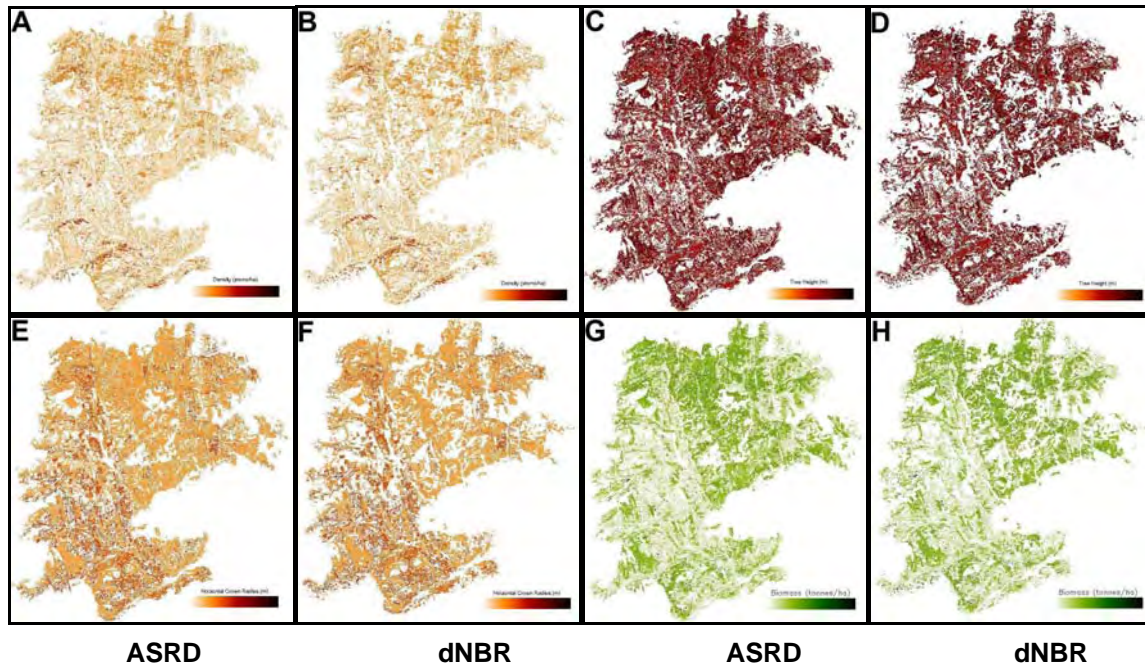
Figure 5. MFM-CRM structural and biomass outputs from pre-fire Landsat imagery, overlaid on ASRD and Landsat dNBR fire maps. Stand density (λ) for ASRD (A) and dNBR (B); Tree height (h+b) for ASRD (C) and dNBR (D); Horizontal crown radius (r) for ASRD (E) and dNBR (F); Above-ground biomass for ASRD (G) and dNBR (H).

Comparison of MFM-ASRD and MFM-dNBR Products

The map outputs for selected MFM-CRM products are shown in Figure 5 for density, horizontal crown radius, tree height (a function of MFM outputs of vertical crown radius and height to crown center), and above-ground biomass. One of the objectives of this first paper was to demonstrate the use of MFM-CRM with both the ASRD map and the Landsat dNBR products. This has been achieved. However, as mentioned earlier, field or other validation of these products was not possible in this study and instead the discussion of results is necessarily limited to spatial pattern analysis (Figure 5) and relative differences (Table 3) only. In future work, validation of these results is planned.

Table 3. Percent (%) difference of MFM-CRM outputs for ASRD vs. Landsat dNBR fire maps.

MFM-CRM Parameter	% difference
Density (λ)	9.61
Horizontal crown radius (r)	10.53
Vertical crown radius (b)	14.22
Height to crown center (h)	13.13
Tree height	13.42
Above ground biomass	16.60

In terms of comparing the ASRD and dNBR spatial patterns of forest structure and biomass (Figure 5), the extent of burned vs. non-burned pixels is directly a function of the fire classes overlaid on each product (i.e. the ASRD and Landsat dNBR maps). Structure and biomass were derived from the full image area (pre-fire) and so this information was available for all pixels throughout the Landsat scene (inside and outside fire). Thus, differences in individual structural parameters and derived products (e.g. biomass) as shown in Figure 5 and Table 3 were due primarily to the structural and biophysical properties of pixels included in the ASRD map but not in the dNBR map (i.e. most, if not all occurrences are unburned pixels that are in the ASRD burn class). In terms of overall magnitude

across the Landsat scene, all MFM-CRM outputs associated with the ASRD map were greater than the dNBR map. The percent differences (Table 3) ranged from 9.6% to 16.6%. This difference was due to the variable structure associated with the unburned pixels that were included in the ASRD burned class. Among the highest relative differences were those associated with derived products (i.e. height as a function of h+b; biomass as a function of MFM-CRM structure and field inputs). This suggests that error propagation occurred in the derivation of these products, interpreted here with respect to the magnitude of relative differences amongst various structural and biophysical outputs.

CONCLUSION

The Landsat satellite-derived differenced Normalized Burn Ratio (dNBR) method of fire mapping was compared with an aerial photo-interpretation based method from the Alberta government (ASRD). The ASRD product had a different, more specific mapping objective that did not require detailed burn delineation but instead tolerated considerable generalization of smaller non-burned areas within large burned polygons. The dNBR method provided a more detailed, per-pixel product from which the fire area estimate was refined (reduced) by over 3500 ha, a relative reduction of 19%. This difference, while appropriately ignored in some applications, more broadly cannot be deemed insignificant, particularly for other uses of these products and in situations involving larger area, regional to national-scale applications where accumulated error would become substantial. More fundamentally, the dNBR method provides a consistent, apparently accurate and robust approach to fire mapping that may be particularly well suited to larger area applications where aerial photo interpretation would be impractical. The dNBR method requirement of pre- and post-fire imagery represents increased cost and reduced likelihood of appropriate scene acquisition (e.g. cloud cover), although as noted in Key and Benson (2006), there is flexibility in terms of appropriate temporal windows for acquiring these images, ranging up to two to three years in the case of Extended Assessments.

Within this context, a physically-based canopy reflectance modeling approach (MFM-CRM) was demonstrated for estimating forest structure and biomass for the purpose of obtaining relevant fire information that could contribute to carbon modeling and fire assessment protocols. The MFM-CRM approach integrated with both the ASRD and dNBR products and an initial assessment of relative differences of forest structure and biomass as a function of these different fire map products was performed. In this first study, no validation data were available and thus a key next step is to acquire that with reference to archival field and Alberta Vegetation Inventory (AVI) information.

ACKNOWLEDGEMENTS

REFERENCES

Achuff, P. I. (1992). Natural regions, subregions and natural history themes of Alberta: a classification for protected areas management. Alberta Environmental Protection. Edmonton, Alberta.

ASRD (2006). Sustainable Resource Development, Government of Alberta. Wildfire Perimeters for the Years 2000 – 2005 vector digital data metadata file. Edmonton, Alberta. (Last accessed Aug. 31, 2007 at: http://www.srd.gov.ab.ca/wildfires/docs/historical_fire_polygons_2000s.zip)

AVI (2006). Alberta Vegetation Inventory, Sustainable Resource Development, Government of Alberta. Edmonton, Alberta. (Last accessed Sept. 4, 2007 at: http://www.srd.gov.ab.ca/lands/geographicinformation/ resourcedataproductcatalogue/avi.aspx)

Brewer, C.K., J.C. Winne, R.L. Redmond, D.W. Opitz and M. V. Mangrich (2005). Classifying and Mapping Wildfire Severity: A Comparison of Methods. *Photogrammetric Engineering & Remote Sensing*, 71(11).

Cahoon Jr., D.R., Pierson, J.M, Stocks, B.J., Levine, J.S., Cofer, I.W.R (1994). Satellite analysis of the severe 1987 forest fire in northern China and Southeast Siberia. *Journal of Geophysical Research*, 99, 18627 – 18638

Chander G., and B. Markham (2003). Revised Landsat-5 TM Radiometric Calibration Procedures and Postcalibration Dynamic Ranges. *IEEE Trans. Geoscience and Remote Sensing*, 41(11):2674 - 2677

Cihlar, J., S. Denning, F. Ahern, O. Anno, A. Belward, F. Bretherton, W. Cramer, G. Dedieu, C. Field, R. Francey, R. Gommes, J. Gosz, K. Hibbard, T. Igarashi, P. Kabat, D. Olsen, S. Plummer, I. Rasool, M. Raupach, R. Scholes, J. Townshend, R. Valentini, and D. Wickland, (2002). Initiative to quantify terrestrial carbon sources and sinks. *EOS Transactions*, American Geophysical Union. 83(1): 1,6-7.

Cihlar, J., B. Guindon, J. Beaubien, R. Latifovic, D. Peddle, M.Wulder, R. Fernandes, J. Kerr, (2003). From Need to Product: A Methodology for Completing a Land Cover Map of Canada using Landsat Imagery. *Canadian Journal of Remote Sensing*. Special Issue on Landsat-7. 29(2): 171-186.

Conrad, S.G., E.P. Davidenko, G.A. Ivanova, A.I. Sukhinin, B.J. Stocks, D.R. Cahoon (2002). Determining effects of area burned and fire severity on carbon cycling and emissions in Siberia. *Climate Change*,55, 197 - 211

Fraser, R.H., and Z. Li (2002). Estimating fire-related parameters in boreal forest using SPOT VEGETATION. *Remote Sensing of Environment*, 82: 95-110

French, N. H. F., P. Goovaerts, and E. S. Kasischke. (2004). Uncertainty in estimating carbon emissions from boreal fires. *Journal of Geophysical Research* 109 (D14S08): doi: 10.1029/2003JD003635.

Gamon, J.A., K.F. Huemmrich, D.R. Peddle, J. Chen, D. Fuentes, F.G. Hall, J. S. Kimball, S. Goetz, J. Gu, K.C. McDonald, J.R. Miller, M. Moghaddam, A.F. Rahman, J.-L. Roujean, E.A. Smith, C.L. Walthall, P. Zarco-Tejada, B. Hu, R.Fernandes and J. Cihlar, (2004). Remote Sensing in BOREAS: Lessons Learned. *Remote Sensing of Environment* BOREAS Special Issue 89(2):139-162.

Irish, R. R. (2000). Landsat 7 Science Data Users Handbook: "Data Products". NASA GSFC. (Last accessed Aug. 31, 2007 at: *http://ltpwww.gsfc.nasa.gov/IAS/handbook/handbook_htmls/chapter11/chapter11.html*)

Jia, G.J., I.C. Burke, A.F.H. Goetz, M.R. Kaufmann and B.C. Kindel (2006). Assessing spatial patterns of forest fuel using AVRIS data. *Remote Sensing of Environment*, 102 (2006) 318-327

Key, C.H., N. Benson, D. Ohlen, S. Howard and Z. Zhu (2003). Data acquisition timing for burned area remote sensing and relationships to measures of burn severity. *2nd Int. Wildland Fire Ecology & Fire Management Congress / 5th Symp. Fire & Forest Meteorology, Orlando, FL., USA*. Nov 16-20 Paper J7G.3

Key, C.H., and N. C. Benson. (2006). *Landscape Assessment: Ground measure of severity, the Composite Burn Index: and remote sensing of severity, the Normalized Burn Ratio*. *In* D.C. Lutes; R.E. Keane; J.F. Caratti; C.H. Key; N.C. Benson; S. Sutherland; and L.J. Gangi. 2006. FIREMON: Fire Effects Monitoring and Inventory System. USDA Forest Service Rocky Mountain Research Station, Ogden, UT. Gen. Tech. Rep. RMRS-GTR-164-CD: LA-51. *(Last accessed* Aug 31, 2007 *at http://frames.nbii.gov/projects/firemon/ FIREMON_LandscapeAssessment.pdf*)

Lentile, L. B., Z. A. Holden, A. M. S. Smith, M. J. Falkowski, A. T. Hudak, P. Morgan, S. A. Lewis, P. E. Gessler, and N. C. Benson (2006). Remote sensing techniques to assess fire characteristics and post-fire effects. *International Journal of Wildland Fire* 15: 319-345.

Li, X. and A.H. Strahler, (1992). Geometric-optical bidirectional reflectance modeling of the discrete crown vegetation canopy: effect of crown shape and mutual shadowing. *IEEE Transactions on Geoscience and Remote Sensing*, 30(2):276-292.

Miller, J.D., and S.R. Yool, (2002). Mapping forest post-fire canopy consumption in several overstory types using multi-temporal Landsat TM and ETM data, *Remote Sensing of Environment*, 82 (2002) 481-496

NACP, (2005). North American Carbon Program Science Implementation Strategy.. Prepared for the U.S. Carbon Cycle Scientific Steering Group (CCSSG) and Interagency Working Group (CCIWG). July 2005. Available at: http://www.nacarbon.org/nacp/

Peddle, D.R., P.M. Teillet and M.A. Wulder, (2003a). Radiometric Image Processing. Chapter 7, in: "*Remote Sensing of Forest Environments: Concepts and Case Studies*" (Eds.: M.A. Wulder and S.E. Franklin) Kluwer Academic Press, London/Dordrecht/Boston (Norwell, Massachusetts, USA). pp.181-208.

Peddle, D.R., S.E. Franklin, R.L. Johnson, M.A. Lavigne and M.A. Wulder, (2003b). Structural Change Detection in a Disturbed Conifer Forest Using a Geometric Optical Reflectance Model in Multiple-Forward Mode. *IEEE Transactions on Geoscience and Remote Sensing* 41(1): 163-166.

Peddle, D.R., J.E. Luther, N. Pilger and D. Piercey, (2003c). Forest biomass estimation using a physically-based 3-D structural modeling approach for Landsat TM cluster labeling, Newfoundland. In, *Proceedings, 25th*

Canadian Symposium on Remote Sensing, Montreal, PQ. Canadian Aeronautics and Space Institute, Ottawa. (CD-ROM)

Peddle, D.R., R.L. Johnson, J. Cihlar and R. Latifovic, (2004). Large Area Forest Classification and Biophysical Parameter Estimation using the 5-Scale Canopy Reflectance Model in Multiple-Forward Mode. *Remote Sensing of Environment* BOREAS Special Issue 89(2):252-263.

Peddle, D.R., R.L. Johnson, J. Cihlar, S.G. Leblanc J.M. Chen and F.G. Hall, (2007). Physically-Based Inversion Modeling for Unsupervised Cluster Labeling, Independent Forest Classification and LAI Estimation using MFM-5-Scale. *Canadian Journal of Remote Sensing* 33(3): 214-225.

Pilger, N., D.R. Peddle and R.J. Hall, (2003). Forest Volume Estimation using a Canopy Reflectance Model in Multiple-Forward-Mode. In, *Proceedings, 25th Canadian Symposium on Remote Sensing*, Montreal, PQ. Canadian Aeronautics and Space Institute, Ottawa. (CD-ROM)

Soenen, S.A., D.R. Peddle and C.A. Coburn, (2005). SCS+C: A Modified Sun-Canopy-Sensor Topographic Correction in Forested Terrain. *IEEE Transactions on Geoscience and Remote Sensing*. 43(9): 2149-2160.

Soenen, S.A., D.R. Peddle, C.A. Coburn, R.J. Hall, and F.G. Hall, (2007a). Improved topographic correction of forest image data using a 3-D canopy reflectance model in multiple forward mode. *International Journal of Remote Sensing*. (in press).

Soenen, S.A. D.R. Peddle, C.A. Coburn, R.J. Hall and F.G. Hall (2007b). Canopy Reflectance Model Inversion in Multiple Forward Mode: Forest Structural Information Retrieval from Solution Set Distributions. *Photogrammetric Engineering and Remote Sensing*, (in press)

Soenen, S.A. D.R. Peddle, R.J. Hall and C.A. Coburn (2007c). Multiple Forward Mode Canopy Reflectance Model Inversion for Above Ground Forest Biomass, Alberta Rocky Mountains. *Proceedings, 28th Canadian Symposium on Remote Sensing / ASPRS Specialty Conference, Ottawa ON. Canada 28 October – 1 Nov. 2007 (these Proceedings.)*

Weber, M.G. and B.J. Stocks (1998) Forest fires and sustainability in the boreal forest of Canada. *Ambio* 27:545-550

Weiss, M., F. Baret, R.B. Myneni, A. Pragnere, Y. Knyazikhin, 2000. Investigation of a Model Inversion Technique to Estimate Canopy Biophysical Variables from Spectral and Directional Reflectance Data, *Agronomie*, 20: 3-22.